Literature Cited

(1) Kamimoto, M.; Sakuta, K; Ozawa, T.; Sakamoto, R. *Circ. Electrotech. Lab.* **1978**, *No. 196*, 10.
(2) Takagi, R.; Shimotake, H. *New Mater. New Processes* **1983**, *2*, 332.
(3) Mikami, M.; Odawara, O.; Kawamura, K. *J. Chem. Eng. Data* **1981**, *26*, 411.
(4) Uchiyama, Y.; Kawamura, K. *J. Chem. Eng. Data* **1981**, *26*, 407.
(5) Stern, K. *J. Phys. Chem. Ref. Data* **1972**, *1*, 747.
(6) King, L. A.; Duke, F. R. *J. Electrochem. Soc.* **1964**, *6*, 712.
(7) Bockris, J. O'M.; Richards, N. E. *Proc. R Soc. London, Ser. A* **1957**, *241*, 44.
(8) Higgs, R. W.; Litovitz, T. A. *J. Acoust. Soc. Am.* **1960**, *32*, 1108.
(9) Cerisier, P.; Finiels, G.; Doucet, Y. *J. Chim. Phys. Phys.-Chim. Biol.* **1974**, *6*, 836.
(10) Bannard, J. E.; Barton, A. F. M. *J. Chem. Soc., Faraday Trans. 1* **1978**, *74*, 153.
(11) Polyakov, V. D.; Beruli, S. H. *Izv. Sekt. Fiz.-Khim. Anal., Inst. Obshch. Neorg. Khim., Akad. Nauk SSSR* **1955**, *26*, 164.
(12) Iwadate, Y.; Okada, I.; Kawamura, K. *J. Chem. Eng. Data* **1982**, *27*, 288.
(13) Bloom, H.; Knaggs, I. W.; Molloy, J. J.; Welch, D. *Trans. Faraday Soc.* **1953**, *49*, 1458.
(14) Robbins, G. D.; Braunstein, J. *J. Electrochem. Soc.* **1969**, *116*, 1218.
(15) Beruli, A. I.; Bergman, A. G. *Izv. Sekt. Fiz. Khim. A* **1954**, *25*, 218.

Received for review May 30, 1984. Accepted October 5, 1984.

Supplementary Material Available: A table of original data on sound velocity in the molten $NaNO_2$–KNO_3 system (2 pages). Ordering information is given on any current masthead page.

Viscosity and Lithium-7 Nuclear Magnetic Resonance Relaxation Time of Concentrated Lithium Nitrate–Ammonia Solutions

Katsuyuki Uchibayashi, Masahito Niibe, and Yoshio Nakamura*

Department of Chemistry, Faculty of Science, Hokkaido University, 060 Sapporo, Japan

The viscosity coefficient and density of concentrated $LiNO_3$–NH_3 solutions (up to 30 mol % $LiNO_3$) have been determined as a function of composition and temperature. The observed viscosity coefficient and its activation energy show a change in composition dependence around 10 mol % $LiNO_3$. The spin–lattice relaxation time of ${}^7Li$ has also been measured and correlated to the present viscosity data.

Introduction

Lithium nitrate ($LiNO_3$) is very soluble in liquid ammonia (NH_3); the saturated solution at room temperature contains about 35 mol % $LiNO_3$. Three compounds, $LiNO_3{\cdot}2NH_3$, $LiNO_3{\cdot}4NH_3$, and $LiNO_3{\cdot}8NH_3$ are known from the study of the phase diagram (*1*). It will be of great interest to study transport phenomena in such concentrated solutions of an ionic solute in a molecular solvent (*2*). No data on the viscosity coefficient of the $LiNO_3$–NH_3 system are available, though the viscosity coefficients of various salt–ammonia systems have been reported by Kikuchi (*3*) many years ago. The purpose of the present study was to determine the viscosity coefficient of the $LiNO_3$–NH_3 system as a function of composition and temperature. The density of this system has also been measured in order to check the existing data (*4*). Measurements have also been made on the spin-lattice relaxation time of ${}^7Li$ in the present system, which is correlated to the results of the viscosity measurements. The present data will serve for better understanding of the transport properties of concentrated electrolyte solutions in polar solvents.

Experimental Section

Material. NH_3 (99.99%, Seitetsu Kagaku Co.) passed through a column with pellets of NaOH was liquefied and treated with lithium metal to remove trace of water and oxygen. It was then distilled over pieces of sodium metal several times and stored in a vessel as a saturated solution of $LiNO_3$. Reagent-grade $LiNO_3$ (Wako Pure Chemical Ltd.) was dried at 110 °C over 24 h and used without further purification. Sample solutions were prepared by distilling purified NH_3 into each measuring cell containing a desired amount of $LiNO_3$ dried under vacuum. The composition of each sample solution was calculated from the weight of the components.

Apparatus and Procedures. The viscosity coefficient of sample solutions was determined with a sealed Ubbelohde type viscometer. The viscometer is about 20 cm in height and has a capillary part of about 8 cm in length, which was immersed in an alcohol bath controlled within ±0.03 °C. The viscosity coefficient η by using the relation

$$\eta = C_1\rho t - C_2\rho/t \tag{1}$$

The constants C_1 and C_2 for each viscometer were determined by using pure methanol with the known values of the viscosity coefficient and density (*5*). The density of sample solutions was determined for some representative compositions by use of a sealed dilatometer whose volume was about 5 cm^3. Estimated errors in ρ, t, and η in the present measurements were ±0.3%, ±0.5%, and ±1%, respectively.

NMR measurements were made with a Bruker SXP 4-100 spectrometer operating at 34.98 MHz for ${}^7Li$. Each sample solution was put into a measuring cell of 8-mm inner diameter. The spin–lattice relaxation time T_1 was measured by using the standard 180°–τ–90° pulse sequence method. Temperatures of samples were controlled within 1 °C by a stream of cooled nitrogen gas.

Results and Discussion

The results for the density, ρ, of the $LiNO_3$–NH_3 system at 20 °C are expressed as

$$\rho(20\ ^\circ\mathrm{C}) = 0.6150 + 2.625X - 2.400X^2\ (\mathrm{g/cm^3}) \tag{2}$$

where X is the mole fraction of the solute ($LiNO_3$). The present results are in good agreement with those given in the literature (*4*). The results at −50 °C are also given by

$$\rho(-50\ ^\circ\mathrm{C}) = 0.7076 + 2.151X - 1.330X^2\ (\mathrm{g/cm^3}) \tag{3}$$

On the other hand, the experimental results for the viscosity coefficient, η, can be expressed by the Andrade equation

$$\log \eta = A/T + B \tag{4}$$

as a function of the absolute temperature T. The experimental values of the constants A and B for each sample solution are

Table I. Viscosity Coefficients of $LiNO_3$-NH_3

$\log \eta = A/T + B$

C_{LiNO_3}, mol %	temp range, °C	η(20 °C), cP	10^3A, K^{-1}	B	E_η, kJ/mol
0	-50 to -30	0.1293[a]	0.3677	-2.1396	7.04
4.71	-50 to -30	0.2713[a]	0.4071	-1.9553	7.79
7.33	-50 to -30	0.3824[a]	0.4946	-2.1047	9.47
9.29	-45 to -25	0.5214[a]	0.5363	-2.1151	10.23
10.35	-50 to -20	0.6272[a]	0.5791	-2.1779	11.09
15.33	-10 to +20	2.328	0.8547	-2.5486	16.36
16.06	-6 to +20	2.859	0.8826	-2.5544	16.90
21.27	0 to +30	8.458	1.3253	-3.5937	25.37
29.15	+15 to +35	29.40	1.5529	-3.8289	29.73

[a] Extrapolated values.

Table II. Relaxation Rates of ^7Li in $LiNO_3$-NH_3

C_{LiNO_3}, mol %	$(1/T_1)_{Li}$, s^{-1}		
	-75 °C	-55 °C	-35 °C
1.03	0.0700	0.0430	0.0312
2.84	0.1126	0.0533	0.0367
5.14	0.1452	0.0766	0.0542
6.59	0.1451	0.0848	0.0598
7.39	0.1872	0.1144	0.0805
10.68		0.1672	0.1103

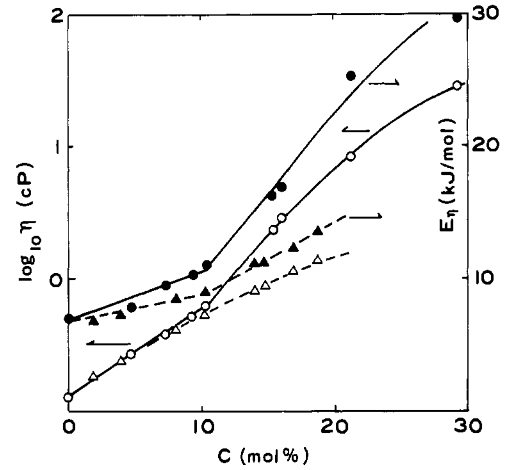

Figure 1. Plot of the logarithm of the viscosity coefficient η at 20 °C and its activation energy E_η vs. mol. percent of solute C: (○, ●) $LiNO_3$-NH_3; (△, ▲) $NaNO_3$-NH_3, ref *3*.

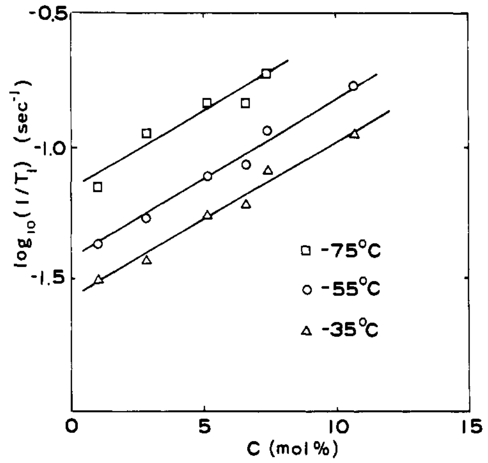

Figure 2. Plot of the logarithm of the spin-lattice relaxation rate $1/T_1$ of ^7Li vs. mol. percent of solute in $LiNO_3$-NH_3.

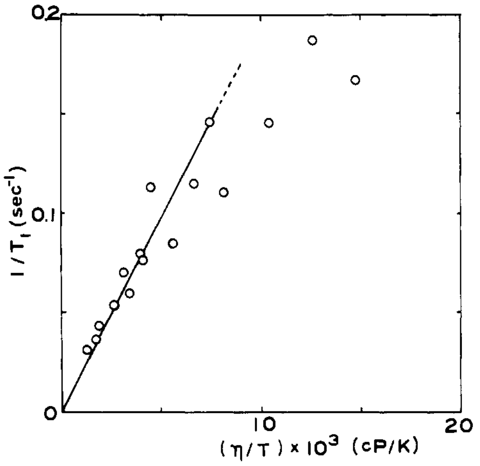

Figure 3. Plot of the spin-lattice relaxation rate $1/T_1$ of ^7Li vs. viscosity coefficient divided by the absolute temperature η/T in $LiNO_3$-NH_3.

summarized in Table I. The results for pure NH_3 are in good agreement with those in the literature (*3, 6*). Figure 1 shows the composition dependence of the viscosity coefficient at 20 °C and the activation energy of viscosity, E_η, calculated from the constant A of eq 4. These results are compared with those of the $NaNO_3$-NH_3 system (*3*) in Figure 1.

In Table II are given the spin-lattice relaxation rates, $1/T_1$, of ^7Li as a function of composition. At a given temperature, the logarithm of $1/T_1$ increases almost linearly with the solute concentration up to 10 mol %, as shown in Figure 2. As a ^7Li nucleus ($I = {}^3/_2$) has an electric quadrupole moment, the nuclear spin relaxation is mainly due to the interaction of the quadrupole moment with electric field gradients present at the position of the nucleus. In the extreme narrowing case, the expression for the relaxation rate is approximately given by (*7, 8*)

$$(1/T_1)_{Li} \cong (1/10)(e^2Qq/\hbar)^2\tau_c \qquad (\text{for } I = {}^3/_2) \qquad (5)$$

where Q is the electric quadrupole moment, q the electric field gradient, and τ_c the correlation time for the quadrupolar interaction. In a monatomic ion, the field gradient is produced by the intermolecular effect, particularly due to the electric dipoles of solvent molecules surrounding the ion. The dominant contribution to τ_c may be the reorientational time of the ammonia molecules in the first coordination sphere, which may be related to the macroscopic viscosity, η, through the Debye equation (*7*)

$$\tau_c = {}^4/_3\pi a^3\eta/k_BT \qquad (6)$$

where a is the molecular hydrodynamic radius, and k_B the Boltzmann constant. Hence, from eq 5 and 6 we have

$$(1/T_1)_{Li} \cong \alpha(\eta/T) \qquad (7)$$

where

$$\alpha = (2/15)\pi a^3(e^2Qq/\hbar^2)^2/k_B \qquad (8)$$

Figure 3 shows the plot of the observed values of $(1/T_1)_{Li}$ against the factor η/T, with the present data for η. Values of η/T were taken for various solutions with different compositions. Though scatter of experimental data is relatively large for larger values of η/T, a linear relation was found and expressed for $\eta/T < 7.5 \times 10^{-3}$ as

$$(1/T)_{Li} = 19.1(\eta/T)\ (s^{-1}) \qquad (9)$$

where η is given in centipoise. This linear relation suggests that the field gradient q and the hydrodynamic radius a of a solvated Li^+ ion do not change significantly with composition and temperature in the relatively low η/T region, implying an invariance of the structure of the first solvation shell of the ion. It is seen in Figure 1 that both the curves for $\log \eta$ and E_η change their slopes around $C \simeq 10$ mol %, where the mole ratio of NH_3 to $LiNO_3$ is about 10. Such a change of the slope of $\log \eta$ and E_η is much less obvious in the $NaNO_3$-NH_3 system, reflecting a relatively weak solute-solvent interaction in this system. In more concentrated solutions above 10 mol %, the simple Debye equation (eq 6) may no longer be valid and much more hindered rotational and translational motion of the solvated Li^+ ion is expected with decreasing the number of solvent molecules (*9*).

Registry No. ^7Li, 13982-05-3; NH_3, 7664-41-7; $LiNO_3$, 7790-69-4.

Literature Cited

(1) "Landort-Börnstein, Teil 2, Band b, Lösungsgleichgewichte I"; Springer-Verlag: Berlin, 1962; p 314.
(2) Richter, J. "Ionic Liquids"; Inman, D., Lovering, D. G., Eds.; Plenum Press: New York, 1981; p 145.
(3) Kikuchi, S. *Kogyo Kagaku Zasshi* **1944**, *47*, 305.
(4) "Landort-Börnstein, Neue Serie IV/Ia, Dichten flüssiger Systeme"; Springer-Verlag: Berlin, 1974; p 16.
(5) "Handbook of Chemistry and Physics", 54th ed.; CRC Press: Cleveland, OH, 1974.
(6) Nozaki, T.; Shimoji, M. *Trans. Faraday Soc.* **1969**, *65*, 1489.
(7) Abragam, A. "The Principles of Nuclear Magnetism"; Clarendon Press: Oxford, 1961.
(8) Geiger, A.; Hertz, H. G. *Adv. Mol. Relaxation Processes* **1976**, *9*, 293.
(9) Nakamura, Y.; Shimokawa, S.; Futamata, K.; Shimoji, M. *J. Chem. Phys.* **1982**, *77*, 3258.

Received for review June 15, 1984. Accepted October 15, 1984.

Solubility Relations in the System Sodium Chloride-Ferrous Chloride-Water between 25 and 70 °C at 1 atm

I-Ming Chou* and Luong D. Phan

U.S. Geological Survey, 959 National Center, Reston, Virginia 22092

Solubility relations in the ternary system $NaCl-FeCl_2-H_2O$ have been determined by the visual polythermal method at 1 atm from 20 to 85 °C along six composition lines. These six composition lines are defined by mixing $FeCl_2·4H_2O$ with six aqueous NaCl solutions containing 5, 10, 11, 15, 20, and 25 wt % of NaCl, respectively. The solid phases encountered in these experiments were NaCl and $FeCl_2·4H_2O$. The maximum uncertainties in these measurements are ±0.02 wt % NaCl and ±0.15 °C. The data along each composition line were regressed to a smooth curve when only one solid phase was stable. When two solids were stable along a composition line, the data were regressed to two smooth curves, the intersection of which indicated the point where the two solids coexisted. The maximum deviation of the measured solubilities from the smoothed curves is 0.14 wt % $FeCl_2$. Isothermal solubilities of halite and $FeCl_2·4H_2O$ were calculated from these smoothed curves at 25, 50, and 70 °C.

Introduction

Hydrated ferrous chloride is an occasional phase found together with halite and/or sylvite in fluid inclusions in quartz in pegmatites (e.g., Naumov and Shapenko (*1*)) and in porphyry systems (e.g., Grant et al. (*2*)). However, data on the solubility of ferrous chloride in geothermal brines do not exist. In this study, the solubility relations in the system $NaCl-FeCl_2-H_2O$ were determined at 1 atm and between 25 and 70 °C.

Experimental Section

The visual polythermal method used in this study has been discussed in detail previously (*3-5*). Solubilities of $FeCl_2·4H_2O$ have been determined between 20 and 75 °C along the two composition lines AL and BL shown in Figure 1, and between 40 and 75 °C along the line CL. Solubilities of halite have been determined between 20 and 85 °C along the lines DL, EL, FL, and GL, and between 20 and 40 °C along the line CL. As an example for the composition line EL, a sample (~12 g) was prepared by mixing weighed amounts of $FeCl_2·4H_2O$ (Fisher, Lot No. 742298) and a stock solution of 15 wt % NaCl (point E in Figure 1) in a Pyrex tube containing a magnetic stirring bar. A layer of silicone oil (~1 cm) was added to seal the tube and prevent water gain or loss. To minimize oxidation of the sample solution during the experiment, the test tube was sealed by a rubber stopper and a stream of H_2 (at ~1 atm) was kept flowing continuously through the cavity above the silicone seal. The assembly was first heated to dissolve most of the solids and then allowed to cool slowly to nucleate a small number of relatively large crystals. The assembly was then mounted in a glycol bath and incrementally heated and vigorously agitated until the last crystal was dissolved. Heating increments were made progressively smaller as the amount of salt decreased. The temperature (read to ±0.1 °C with a calibrated platinum resistance thermometer) at which the last crystal disappeared was taken as the equilibrium temperature for the bulk composition in the tube. Once the last crystal dissolved, the solution had to be significantly supercooled to induce crystallization. This phenomenon precludes the possibility of reversing the solubility data by simple cooling. However, the equilibrium between crystals and solution in the heating experiments has been sufficiently demonstrated (*3*).

Results and Discussion

Weighing $FeCl_2·4H_2O$ directly out of the bottle, although convenient, might introduce extra uncertainties into the experiment. The magnitude of these uncertainties was estimated by coulometrically titrating Cl^- in a 10.00 wt % $FeCl_2$ solution prepared in the same fashion. Duplicate analyses gave 9.89 ± 0.04 wt % $FeCl_2$. The system used for solubility measurements was also calibrated by determining the solubility of $FeCl_2·4H_2O$ in the binary system $FeCl_2-H_2O$ and comparing the results (Table I) with those reported by Schimmel (*6*) (Figure 2). It is clear from Figure 2 that our data agree very well with those of Schimmel at temperatures above 40 °C. Below 40 °C, however, our data show that $FeCl_2·4H_2O$ is slightly less soluble. The discrepencies at lower temperatures can be attributed to the scattering of Schimmel's data but not to the uncertainties involved in weighing $FeCl_2·4H_2O$ in this study, since